LHX2 is a direct NF-{kappa}B target gene that promotes primary hair follicle placode down-growth

Tomann, P., Paus, R., Millar, S.E., Scheidereit, C., Schmidt-Ullrich, R.

Development
2016 MAY 03 ; 143(9): 1512-1522
doi: 10.1242/dev.130898
Publisher: The Company of Biologists Ltd

© 2016. Published by The Company of Biologists Ltd | Development (2016) 143, 1512-1522 doi:10.1242/dev.130898

RESEARCH ARTICLE

Lhx2 is a direct NF-κB target gene that promotes primary hair follicle placode down-growth

Philip Tomann[1], Ralf Paus[2,3], Sarah E. Millar[4], Claus Scheidereit[1] and Ruth Schmidt-Ullrich[1,*]

ABSTRACT

In the epidermis of mice lacking transcription factor nuclear factor-kappa B (NF-κB) activity, primary hair follicle (HF) pre-placode formation is initiated without progression to proper placodes. NF-κB modulates WNT and SHH signaling at early stages of HF development, but this does not fully account for the phenotypes observed upon NF-κB inhibition. To identify additional NF-κB target genes, we developed a novel method to isolate and transcriptionally profile primary HF placodes with active NF-κB signaling. In parallel, we compared gene expression at the same developmental stage in NF-κB-deficient embryos and controls. This uncovered novel NF-κB target genes with potential roles in priming HF placodes for down-growth. Importantly, we identify *Lhx2* (encoding a LIM/homeobox transcription factor) as a direct NF-κB target gene, loss of which replicates a subset of phenotypes seen in NF-κB-deficient embryos. *Lhx2* and *Tgfb2* knockout embryos exhibit very similar abnormalities in HF development, including failure of the E-cadherin suppression required for follicle down-growth. We show that TGFβ2 signaling is impaired in NF-κB-deficient and *Lhx2* knockout embryos and that exogenous TGFβ2 rescues the HF phenotypes in *Lhx2* knockout skin explants, indicating that it operates downstream of LHX2. These findings identify a novel NF-κB/LHX2/TGFβ2 signaling axis that is crucial for primary HF morphogenesis, which may also function more broadly in development and disease.

KEY WORDS: NF-κB, LHX2, Hair follicle, TGFβ2, Cell migration, E-cadherin, EDA-A1, EDAR, Mouse, Embryo, Placode, Stem cell

INTRODUCTION

Hair follicle (HF) development is initiated by a reciprocal signaling interplay between the surface epithelium and the underlying mesenchyme that results in local epithelial thickenings, the HF placodes (Biggs and Mikkola, 2014; Fuchs, 2007; Hardy, 1992; Schmidt-Ullrich and Paus, 2005; Schneider et al., 2009; Sennett and Rendl, 2012). The regular array of placodes is thought to be mediated by a reaction-diffusion system of competing placode activator and inhibitor morphogens (Bazzi et al., 2007; Jiang et al., 2004; Mou et al., 2006; Sick et al., 2006). Mouse HF development occurs in three major waves, with primary (guard, tylotrich) HFs forming at embryonic day (E) 14.5, and awl/auchene and zigzag HFs starting to generate at E16.5 and E18.5, respectively. These distinct waves are differentially regulated at the molecular level. Epidermal and dermal canonical WNT/β-catenin signaling is required to initiate the development of all hair types, whereas bone morphogenetic protein (BMP) signals generally function to impede placode development (Andl et al., 2002; Botchkarev et al., 1999; Chen et al., 2012; Mou et al., 2006; Oro and Scott, 1998; Zhang et al., 2008, 2009a). In addition to WNT/β-catenin signaling, primary HF formation specifically depends on the activity of the TNF family member EDA-A1 (ectodypslasin-A1; also known as EDA) in the epidermis (Headon and Overbeek, 1999; Kere et al., 1996; Laurikkala et al., 2002; Schmidt-Ullrich et al., 2001, 2006). *Eda-A1* ligand and its receptor *Edar* (ectodysplasin receptor) are both direct target genes of WNT/β-catenin, and EDA-A1-EDAR interaction results in downstream activation of the transcription factor nuclear factor-kappa B (NF-κB) in developing primary placodes (Kumar et al., 2001; Laurikkala et al., 2002; Schmidt-Ullrich et al., 2006; Yan et al., 2000; Zhang et al., 2009a).

In the absence of EDA-A1/EDAR/NF-κB signaling, WNT/β-catenin initiates HF placode formation in a messy pre-pattern up to the pre-placode stage (hair morphogenesis stage 0/1; Paus et al., 1999) in which a subset of placode markers is already expressed, but subsequent down-growth and morphogenesis are arrested (Schmidt-Ullrich et al., 2006; Zhang et al., 2009a). The ill-defined borders of these pre-placodes revealed a role for EDA-A1/EDAR/NF-κB signaling in pattern refinement of early WNT/β-catenin activity in primary HF placodes by upregulating expression of WNT inhibitors such as DKK4 (Bazzi et al., 2007; Fliniaux et al., 2008; Zhang et al., 2009a). Furthermore, a suggested function for EDA-A1/EDAR/NF-κB in suppressing placode-inhibitory BMP signals within primary placodes might be important to maintain HF fate and prevent premature differentiation (Mou et al., 2006; Pummila et al., 2007). With the exception of recombinant Fc-EDA-A1, TNFα and to some extent high doses of the BMP inhibitor noggin, other potential effectors downstream of EDA-A1 signaling, such as SHH or the chemokines CXCL10 and 11, failed to rescue primary HF placode formation in EDA-A1-deficient embryonic skin explants (Laurikkala et al., 2002; Lefebvre et al., 2012; Pummila et al., 2007; Schmidt-Ullrich et al., 2006). This indicates that the known EDA-A1/EDAR/NF-κB target genes are not sufficient to define the apparently complex role of EDA-A1/EDAR/NF-κB signaling in primary hair placode development. Therefore additional NF-κB-dependent factors must be required to establish proper conditions for placode down-growth beyond initiation, patterning and BMP inhibition.

Previous microarray analyses have identified some NF-κB target genes. However, all these studies utilized either whole skin (epidermis and dermis) or skin explants that had been treated with recombinant EDA-A1 or left untreated (Bazzi et al., 2007; Cui et al., 2002, 2006; Laurikkala et al., 2002; Lefebvre et al., 2012; Mou et al., 2006; Pummila et al., 2007). Therefore, placode-specific genes that are expressed at low levels might have been missed. To

[1]Department of Signal Transduction in Tumor Cells, Max-Delbrück-Center (MDC) for Molecular Medicine, Berlin 13092, Germany. [2]Department of Dermatology, University of Münster, Münster 48149, Germany. [3]Dermatological Science Research Group, Centre for Dermatology Research, Institute of Inflammation and Repair, University of Manchester, Manchester M13 9PL, UK. [4]Departments of Dermatology and Cell and Developmental Biology, Perelman School of Medicine, University of Pennsylvania, Philadelphia, PA 19104, USA.

*Author for correspondence (rschmidt@mdc-berlin.de)

Received 11 September 2015; Accepted 19 February 2016

Development (2016) 143, 1512-1522 doi:10.1242/dev.130898

identify additional genes functioning downstream of NF-κB, we established a gene signature that is both placode keratinocyte specific, and NF-κB dependent. To this end, we generated a novel NF-κB-EGFP reporter mouse line. This allowed us to isolate and purify hair placode keratinocytes and to set up a detailed gene expression profile specifically of NF-κB-active primary hair placodes. In parallel, to identify NF-κB-dependent genes, we profiled gene expression in NF-κB-inhibited compared with control embryonic mouse epidermis.

HF placode formation and down-growth is a complex process that depends on changes in local keratinocyte adhesion, migration, polarity and proliferation, as well as modifications in the surrounding extracellular matrix (ECM). In addition to expected NF-κB targets, such as genes that control NF-κB and WNT signaling, we identified a significant number of new targets, including ECM components, genes involved in cell adhesion and migration, and stem cell-associated genes. Of particular interest, we identified the gene encoding the LIM-homeodomain transcription factor LHX2 as a novel NF-κB target gene in HF placodes. LHX2 was originally shown to control patterning, cell fate decisions and axon guidance during embryonic brain development (Bulchand et al., 2001; Hirota and Mombaerts, 2004; Mangale et al., 2008; Porter et al., 1997; Shetty et al., 2013). However, LHX2 also plays an important role in HF stem cell growth and maintenance within the stem cell niche by regulating cell adhesion and cytoskeletal dynamics (Folgueras et al., 2013; Rhee et al., 2006). A requirement of LHX2 for anagen induction has been indicated as well (Törnqvist et al., 2010). LHX2 is expressed in stage 0 and stage 1 embryonic HF placodes that also display NF-κB activity, and *Lhx2*-deficient embryos have reduced numbers of HFs (Rhee et al., 2006; Törnqvist et al., 2010). These data suggest a role for LHX2 in HF morphogenesis. However, as *Lhx2*-deficient embryos die around E15-E16, when primary HF development is still ongoing, further detailed morphological and molecular analyses of HF development have not previously been pursued (Porter et al., 1997; Rhee et al., 2006). A more recent study using a mouse line harboring a hypomorphic *Lhx2* allele examined HF development at later time points, but only confirmed previous assumptions regarding a possible role of LHX2 in HF development (Törnqvist et al., 2010). Our results now demonstrate an essential role for LHX2 in preparing primary hair pre-placodes for down-growth downstream of EDA-A1/EDAR/NF-κB signaling.

RESULTS

NF-κB-dependent gene signature in primary HF placodes reveals a multifunctional role for NF-κB in HF development

To obtain a gene signature for NF-κB-active primary HF placodes, we generated an NF-κB-responsive reporter mouse line that uses EGFP as read-out for *in vivo* NF-κB activity (*κ-EGFP*; Fig. 1A; Table S1). The expression pattern of EGFP was identical to that observed in a previously produced NF-κB reporter line (Schmidt-Ullrich et al., 2001, 1996), including strong NF-κB activity in developing HF placode keratinocytes (Fig. 1A; Fig. S1A). Epidermis from E14.5 *κ-EGFP* embryos was harvested, EGFP-expressing HF placode keratinocytes were purified by fluorescence-activated cell sorting (FACS), and total placode keratinocyte RNA was processed for microarray analysis (Fig. 1B,C; Fig. S1B; Table S1). To exclude contamination of our epidermal samples with mesenchymal cell types, we analyzed mRNA expression of four dermal markers, *Bmp4*, *Col1a1* (collagen 1 alpha1), *Irx1* (Iroquois homebox 1) and *Ngfr* (nerve growth factor receptor; also known as p75NTR), which either revealed absence (*Col1a1*, *Ngfr*) or very low expression levels (*Bmp4*, *Irx1*) of these markers (Fig. S2A) (see http://hair-gel.net/; Botchkareva et al., 1999; St-Jacques et al., 1998). The resulting NF-κB-active placode-specific gene signature was aligned with an epidermis-specific NF-κB-dependent gene signature that was obtained from microarray transcriptional profiling of epidermis from embryos with suppressed NF-κB activity (*ΔN*) compared with littermate controls at E14.5 (Table S2). These experiments allowed us to identify 74 genes that are specifically expressed in NF-κB-active placode cells, and are directly or indirectly dependent on NF-κB signaling (Fig. 1B).

We validated the data from our profiling experiments by comparison with previously described NF-κB targets and functions in the context of HF formation, confirming the sensitivity and specificity of our experimental strategy (Fig. 1C). These genes included those in the SHH signaling pathway (*Shh*, *Gli1*, *Ptch2*, *Etv4* and *Etv5*); known NF-κB target genes such as the NF-κB family member *RelB* (Table S1), *Tnfaip3* (encoding the ubiquitin editing enzyme A20), *Tnf* (TNFα), *Ltb* (lymphotoxin β), *Foxi3* (forkhead box I3), chemokine *Cxcl11*; and regulators of the WNT pathway, such as *Dkk4* and also a newly identified NF-κB target, *Wif1* (WNT inhibitory factor 1) (Fig. 1C; Fig. S3A-C) (Bazzi et al., 2007; Cui et al., 2006; Fliniaux et al., 2008; Lefebvre et al., 2012; Lettice et al., 2012; Mao et al., 2009; Schmidt-Ullrich et al., 2006; Shirokova et al., 2013; Zhang et al., 2009a,b). A striking number of genes that we identified as potential NF-κB target genes encode ECM components [*Frem1* (FRAS1 related extracellular matrix 1), *Mmp9* (metalloproteinase 9), *Tnc* (tenascin C)], receptors and genes implicated in cell migration [*Prokr2* (prokineticin receptor 2), *Nrp2* (neuropilin 2), *Cd74* (HLA class II histocompatibility antigen gamma chain or HLA-DR antigen-associated invariant chain; which can act as a receptor for macrophage migration inhibitory factor)] or are involved in cell-adhesion, such as *Ncam1* and *Madcam1* (Fig. 1C). Although *Frem1*, *Madcam1* and *Mmp9* have previously been described as NF-κB target genes (Takeuchi and Baichwal, 1995; Yoon et al., 2012; Yoshizaki et al., 1998), *Prokr2*, *Nrp2*, *Cd74* and *Ncam1* are new potential targets. Importantly, novel NF-κB-regulated genes with special relevance for hair biology, such as transcription factors *Lhx2* (LIM homeobox protein 2) (Folgueras et al., 2013; Mardaryev et al., 2011; Rhee et al., 2006; Törnqvist et al., 2010), *Sox9* (SRY-box 9) (Nowak et al., 2008; Vidal et al., 2005), *Trps1* (trichorhinophalangeal syndrome 1) (Fantauzzo et al., 2008a,b; Kunath et al., 2002; Malik et al., 2002; Momeni et al., 2000) and *Sox21* (SRY-box 21) (Kiso et al., 2009), were also identified (Fig. 1C). A role for LHX2 in primary HF placode down-growth will be described in more detail below.

A number of previously suggested or confirmed NF-κB target genes were upregulated in HF placodes at E14.5, but were not significantly controlled by NF-κB at this time point (Fig. 1C). These comprised the BMP signaling regulator *Ctgf* (connective tissue growth factor) (Pummila et al., 2007), *Wnt10b* (Zhang et al., 2009a) and bona fide NF-κB target *Nfkbia* (NF-κB inhibitor of κBα, IκBα) (Le Bail et al., 1993). *Ctgf* expression might also be regulated by WNT/β-catenin, which is very active in HF placodes at E14.5. For *Wnt10b*, we showed previously that it is only regulated by NF-κB at E15.5 when primary HF stage 1 placodes enter the germ stage (stage 2) (Zhang et al., 2009a). *Nfkbia* was expected to be downregulated in *ΔN* embryos, but the lack of differential regulation might be due to detection of the truncated human IκBα (ΔN) by the mouse array used for our analysis (Schmidt-Ullrich et al., 2001, 2006).

To verify placode-specific expression and dependence on NF-κB activity, candidate targets were examined by quantitative real time-PCR (qRT-PCR) for enrichment in developing primary HF placodes and for differential expression in *ΔN* versus control epidermis at

Development (2016) 143, 1512-1522 doi:10.1242/dev.130898

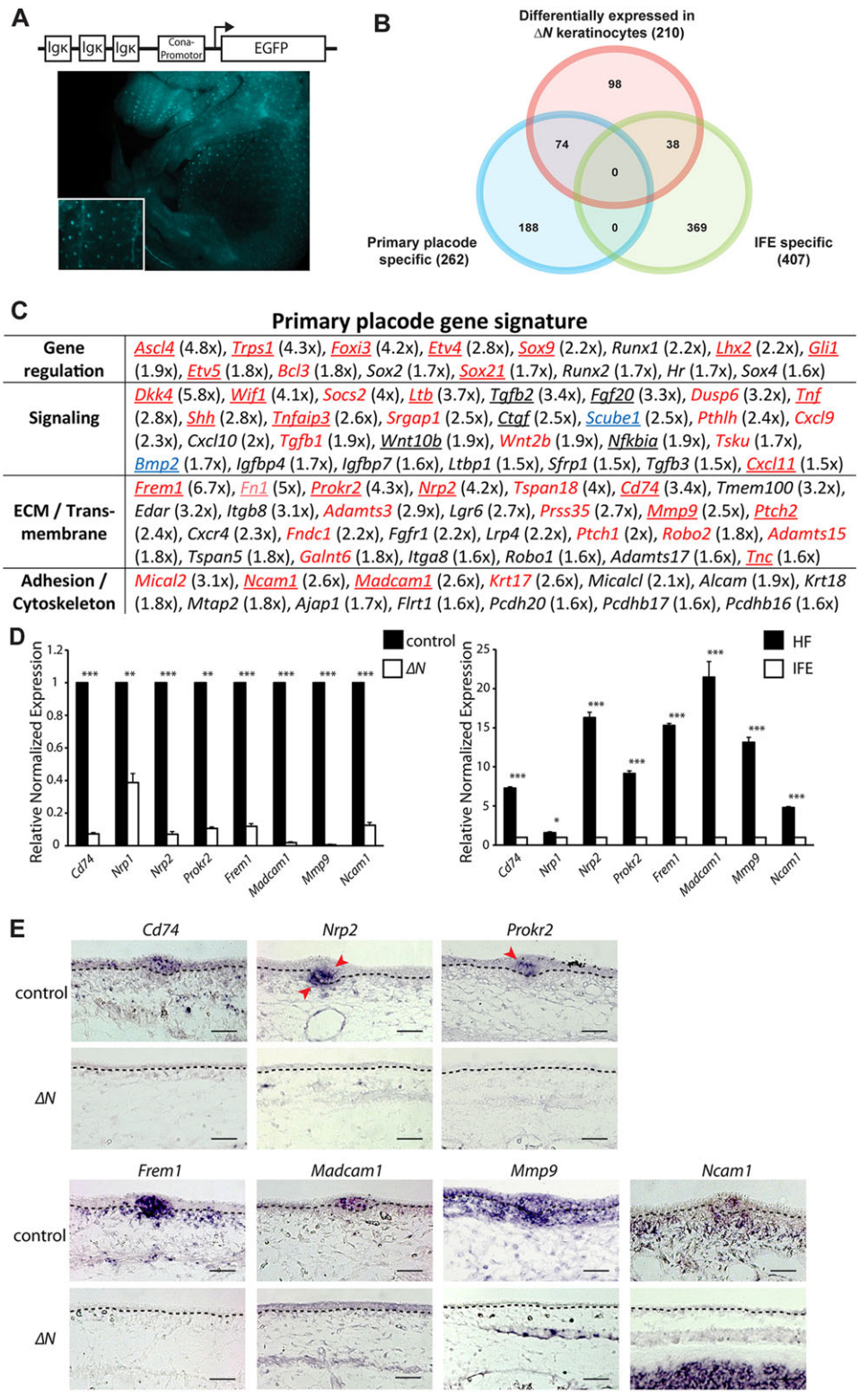

Fig. 1. NF-κB-dependent gene signature in primary HF placodes reveals a multifunctional role. (A) Generation of an NF-κB-responsive EGFP reporter mouse line (*κ-EGFP*). EGFP expression was observed in the developing HF and in blood vessels of the skin at E14.5. Inset shows high magnification of skin with EGFP-expressing placodes. (B) Venn diagram illustrating overlap of genes up- or downregulated in primary HF placodes with differentially expressed genes in *ΔN* versus control epidermal keratinocytes. For full list of microarray data, see Table S1. (C) Primary HF placode-specific gene signature obtained from microarray analysis of sorted EGFP-positive keratinocytes at E14.5. Genes mentioned in the text are underlined. Functional categories with representative examples of mRNAs upregulated ≥1.5× are listed. Fold differences between placodes and interfollicular epidermis (EGFP negative) are indicated in parentheses. Genes highlighted in red were downregulated and in blue upregulated in *ΔN*-positive epidermal keratinocytes. Genes in black were specifically enriched in HF placodes, but not regulated by NF-κB in a significant manner. Note that *Fn1* (in light red) expression is enriched 5× in HF placodes, but is only weakly downregulated in *ΔN* versus controls (~1.3×). (D) Quantitative real-time PCR (qRT-PCR) analysis using either RNA samples from epidermal keratinocytes of $n=3$ control or *ΔN* embryos at E14.5 (left graph), or from FACS-sorted EGFP-positive (HF) or EGFP-negative (IFE) keratinocytes of *κ-EGFP* embryos at E14.5 (right graph). Statistical analyses were performed using a two-tailed unpaired *t*-test. Data are presented as mean±s.e.m. *$P<0.05$; **$P<0.01$; ***$P<0.001$. (E) *In situ* hybridization for the indicated mRNA probes using sagittal skin sections of $n=3$ control and *ΔN* embryos at E14.5. Arrowheads indicate expression in HF placodes and dermal papilla (Nrp2); dashed line delineates the dermal-epidermal boundary. Scale bars: 50 µm.

E14.5 (Fig. 1D; Fig. S3). qRT-PCR revealed a significant dependence on NF-κB activity for all candidate target genes, including those that regulate cell migration and adhesion (Fig. 1D,E; Fig. 3; Fig. S3A,B). To identify potential direct targets, the genomic regions of differentially expressed genes were screened for putative NF-κB-binding sites using the JASPER database (http://jaspar.genereg.net/). We also used the ECR browser (http://ecrbrowser.dcode.org) to check for NF-κB-binding site conservation across species (Table S3). These analyses verified that 96% of the potential target genes contained at least one conserved NF-κB-binding site (Table S3). Potential binding sites were further confirmed by chromatin immunoprecipitation (ChIP) for *Lhx2*, *Sox9*, *Trps1* and *Mmp9* (see below; data not shown; see also Table S3 and supplementary Materials and Methods). Interestingly, 57% of the NF-κB-regulated genes found in our gene chip analysis were also identified by ChIP as direct NF-κB targets in Hodgkin lymphoma

Development (2016) 143, 1512-1522 doi:10.1242/dev.130898

cell lines (de Oliveira et al., 2016) (Table S3). This suggests that physiological NF-κB functions required for primary HF placode formation in mice may in part contribute to human tumor growth and/or survival.

HF placode-specific mRNA expression of identified potential NF-κB target genes was further validated by *in situ* hybridization (ISH) on control skin and *ΔN* skin samples at E14.5 (Fig. 1E; Fig. S3C). Interestingly, mRNA expression of *Bmp2* and *Scube1* (signal peptide-CUB domain EGF-related 1), a potential SHH and BMP signaling regulator (Johnson et al., 2012; Tsao et al., 2013), was expanded in the absence of epidermal NF-κB activity. ISH revealed that *Bmp2* and *Scube1* were ubiquitously expressed in the epidermis of *ΔN* embryos at E14.5, whereas expression was restricted to primary HF placodes in controls (Fig. S3C). This suggests that NF-κB activity might be indirectly required for restricting *Bmp2* and *Scube1* expression to HF placodes. Some of the NF-κB-regulated genes were also expressed in the dermal condensate (*Nrp2*, *Mmp9*, *Tnc*) and at the interface between placode and dermal condensate (*Mmp9*, *Tnc*) (Fig. 1E; Fig. S3C). This latter group of differentially regulated genes strongly points to a role for NF-κB in ECM modulation and in cell migration in order to allow placode down-growth, and further suggests additional non-cell-autonomous mechanisms by which epithelial NF-κB signaling modulates gene expression in other cell types. Note that six genes were specifically upregulated in the interfollicular epidermis (IFE), but downregulated by NF-κB in placodes (Table S4). However, none of these genes has any known functions in IFE development or maintenance, suggesting that NF-κB is not required for downregulating important IFE regulatory genes in order to promote HF formation.

NF-κB directly regulates *Lhx2* expression and acts in concert with LHX2 to control genes involved in cell migration during placode down-growth

Although the novel NF-κB targets *Lhx2* and *Sox9* may suggest an interesting role for NF-κB in stem cell biology, these HF stem cell markers have not previously been associated with early stages of placode formation. mRNA expression of *Lhx2* and *Sox9* was strictly dependent on NF-κB activity in primary HF placodes at E14.5 (Fig. 2A; Fig. S3A-C). In line with this, the promoter of each of

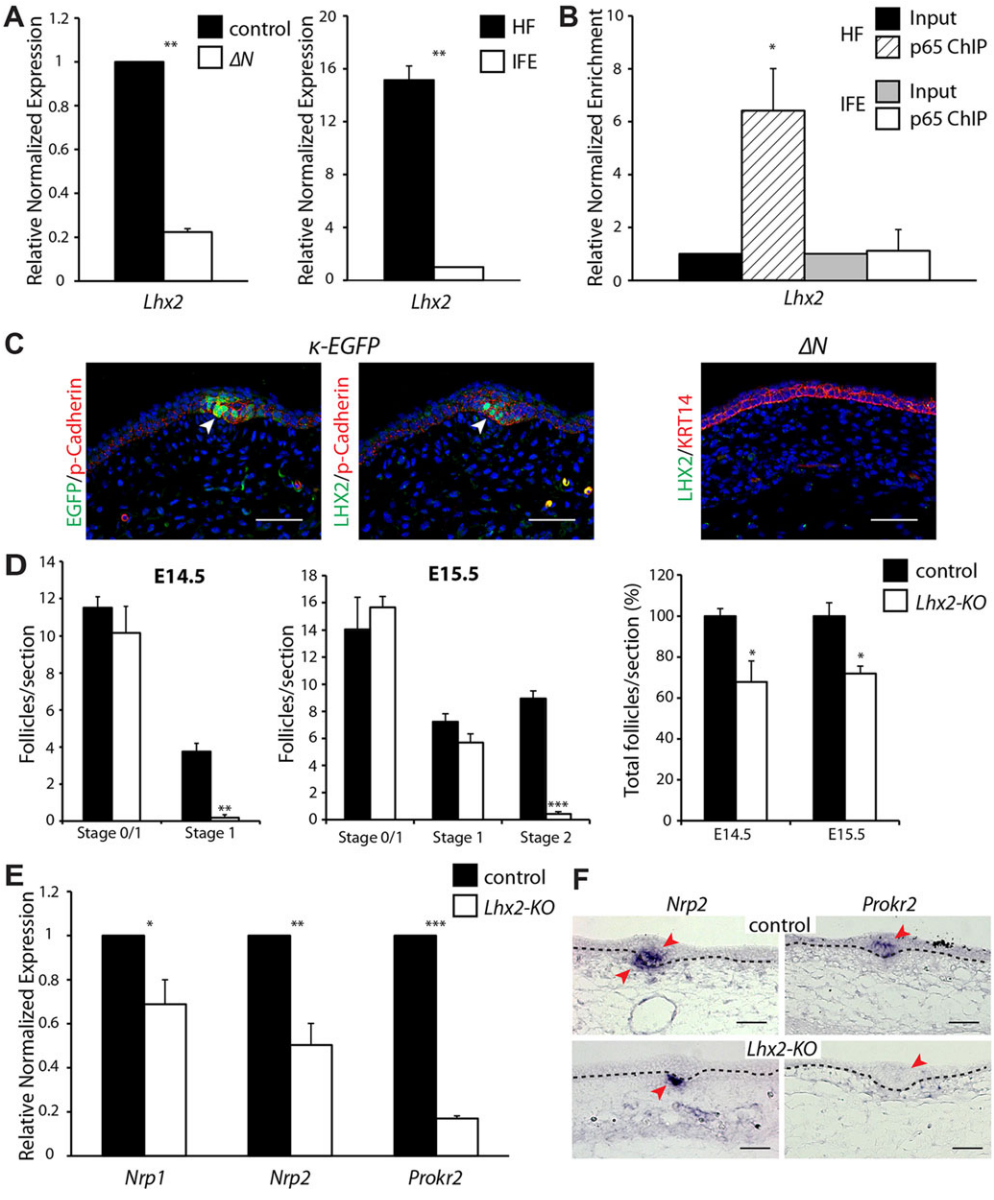

Fig. 2. *Lhx2* is a direct target gene of NF-κB during primary placode formation and acts in concert with NF-κB to regulate genes involved in cell migration. (A) qRT-PCR of *Lhx2* mRNA expression from epidermal keratinocytes of *n*=3 control or *ΔN* embryos (left graph), or from EGFP-positive placode and EGFP-negative IFE keratinocytes (right graph) at E14.5. (B) NF-κB p65-specific ChIP assays using EGFP-positive placode and EGFP-negative IFE keratinocyte extracts from *κ-EGFP* embryos at E14.5, and *Lhx2* and control *Gapdh* primers. (C) Immunostaining on serial sagittal back skin sections of *n*=3 *κ-EGFP* and *ΔN* mice at E14.5 using antibodies against EGFP, P-cadherin (cadherin 3), LHX2 and KRT14. Arrowheads indicate expression in HF placodes. Blue, nuclear DAPI staining. (D) Analysis of primary HF development in *Lhx2*-KO mice revealed a dramatic reduction of stage 1 (E14.5; left graph) and stage 2 (E15.5; middle graph) primary HF. Overall primary HF density in *Lhx2*-KO embryos at E14.5 and E15.5 was reduced by ~30% (right graph). The graphs show quantification from multiple back skin sections of three biological replicates. (E) qRT-PCR for selected NF-κB target genes involved in cell migration using mRNA isolated from epidermal keratinocytes of either *Lhx2*-KO or control embryos at E14.5. (F) *In situ* hybridization for *Nrp2* and *Prokr2* mRNA on sagittal skin sections of control and *Lhx2*-KO embryos at E14.5. Arrowheads indicate mRNA expression in HF placodes and also in the dermal papilla for Nrp2; dashed line delineates dermal-epidermal boundaries. Scale bars: 50 µm. All statistical analyses (A,B,D,E) were performed using two-tailed unpaired *t*-test. Data are presented as mean±s.e.m. **P*<0.05; ***P*<0.01; ****P*<0.001.

Development (2016) 143, 1512-1522 doi:10.1242/dev.130898

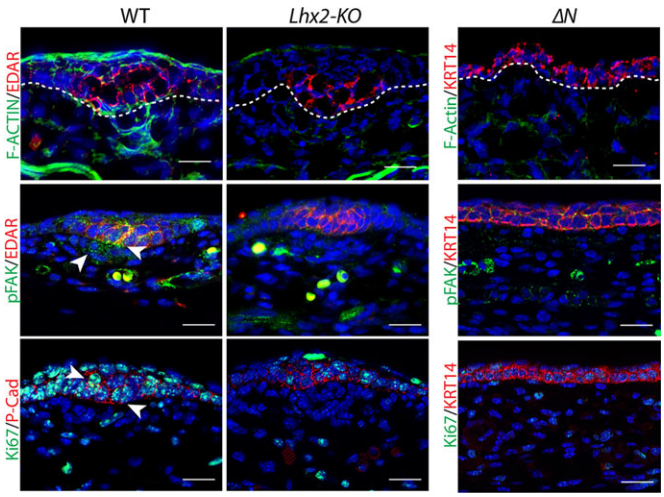

Fig. 3. *ΔN* and *Lhx2*-KO mice exhibit keratinocyte migratory and proliferative defects in the down-growing primary HF placode. Immunostaining on sagittal sections of *n*=3 control, *Lhx2*-KO and *ΔN* embryos at E14.5. Cytoskeletal organization and dynamics (F-actin labeled by Phalloidin), and phosphorylation of FAK (pFAK) were used as markers for cell migration. As readout for proliferation Ki67 expression was used. Antibodies against P-cadherin and EDAR (both red) were used to differentiate HF placodes. Arrowheads indicate Ki67 expression in HF placodes; dashed line delineates dermal-epidermal boundaries. Blue, nuclear DAPI staining. Scale bars: 20 µm.

these genes contains a single NF-κB-binding site that was verified by ChIP (Fig. 2B; data not shown). Although we observed *Sox9* mRNA expression in suprabasal cells of primary HF placodes at E14.5 (Fig. S3C), SOX9 protein expression is not detected prior to E15.5 and does not play a role in HF induction and early morphogenesis, instead being required for formation and maintenance of early and adult bulge stem cells (Kadaja et al., 2014; Nowak et al., 2008; Vidal et al., 2005). We therefore focused on LHX2, as LHX2 protein was readily detected in control HF placodes, was congruent with NF-κB activity, and was absent in the epithelium of *ΔN* embryos at E14.5 (Fig. 2C).

To examine the precise role of LHX2 in HF morphogenesis, we examined primary guard hair placode formation in *Lhx2* knockout (*Lhx2*-KO) embryos at E14.5 and E15.5 compared with control littermates. A previous analysis of *Lhx2*-KO embryos revealed a 40% reduction of developing placodes at E16.5, when secondary HF induction sets in (Rhee et al., 2006). Similarly to *ΔN* embryos, *Lhx2*-KO embryos initiated primary HF pre-placode generation at E14.5 (Fig. 2D) (Schmidt-Ullrich et al., 2006; Zhang et al., 2009a). However, subsequent placode formation went on to stage 1, when most placodes seemed to be arrested (Fig. 2D). Direct LHX2 target genes that are involved in cell adhesion and cytoskeletal dynamics in the HF stem cell niche suggest a possible role for LHX2 in directed cell growth (Folgueras et al., 2013). In line with this, qRT-PCR showed that mRNA expression of genes involved in cell migration, such as the previously identified LHX2 target gene *Nrp1* (Folgueras et al., 2013) as well as the novel NF-κB-regulated genes *Nrp2* and *Prokr2*, were markedly downregulated in the epidermis of *Lhx2*-KO embryos at E14.5 (Fig. 2E). This was further supported by the lack of *in vivo* mRNA expression of *Nrp2* and *Prokr2* in placodes of *Lhx2*-KO embryos compared with controls at E14.5 (Fig. 2F). Again, a possible contamination of dermal cells in purified epidermal cell samples of *Lhx2*-KOs and controls was ruled out by analyzing mRNA expression of *Bmp4*, *Col1a1*, *Irx1* and *Ngfr* (Fig. S2B). However, expression of *Nrp2* mRNA was conserved in the dermal condensate, indicating that *Nrp2* expression is differentially regulated in HF placodes and dermal condensates (Fig. 2C,F). Notably, both *Nrp2* and *Prokr2* genes have potential NF-κB- and LHX2-binding sites in their promoter regions (Table S3), suggesting that these genes might be regulated synergistically by NF-κB and downstream LHX2.

Lhx2-KO and *ΔN* mice display cell migratory and proliferative defects in down-growing primary HF placodes

To explore further whether NF-κB and LHX2 cooperate in regulating directed placode keratinocyte migration and proliferation, we examined staining for F-actin (filamentous actin), phospho-FAK (pFAK; activated focal adhesion kinase) and Ki67 (also known as MKI67) on skin sections at E14.5 (Fig. 3). FAK (also known as PTK2), a non-receptor tyrosine kinase, regulates focal cell adhesion and directed migration, as well as polarity and proliferation (Frame et al., 2010; Schaller, 2010). FAK is stimulated by growth factors, such as platelet-derived growth factor and epidermal growth factor, and by integrin-ECM interactions, which lead to activation of FAK by phosphorylation (Sieg et al., 2000). FAK is essential for embryonic development and also plays an important role in epithelial oncogenesis (reviewed by Sulzmaier et al., 2014). Moreover, mice deficient in epidermal FAK lack proper HF down-growth and display hair cycle defects (Essayem et al., 2006; Schober et al., 2007). F-actin staining is also typically enhanced during directed cell migration. As expected, primary HF placodes of controls displayed pFAK and F-actin staining in the proximal placode border adjacent to the dermal condensate at E14.5 (Fig. 3). However, F-actin and pFAK were absent in the epithelium of *Lhx2*-KOs and *ΔN* embryos (Fig. 3). The proliferation marker Ki67 was also expressed in HF placodes of controls but was not detected in *Lhx2*-KO or *ΔN* embryos at E14.5 (Fig. 3). These data strongly suggest that NF-κB and downstream LHX2 are required to generate the appropriate environment for primary HF placode keratinocytes to proliferate and migrate into the underlying dermis.

Lhx2-KO and *ΔN* mice show impaired TGFβ signaling and lack of E-cadherin downregulation

In order to allow placode down-growth, cells at the very proximal border of the HF placode have to undergo a number of changes, including loss of cell adhesion. This involves local downregulation of the epithelial cadherin E-cadherin (cadherin 1), which forms the transmembrane core of adherens junctions (AJ) (Jamora et al., 2003, 2005). The TGFβ family of signaling molecules controls cell-cell interactions, cell migration and proliferation. In particular, TGFβ2 promotes HF morphogenesis by inducing expression of the transcriptional repressor Snail (SNAI1) and mitogen-activated protein kinase activity, resulting in local E-cadherin downregulation (Jamora et al., 2005). Mice lacking TGFβ2 activity display a delay in HF development and a 50% reduction in the numbers of follicles that form (Foitzik et al., 1999; Jamora et al., 2005). These studies only examined secondary HF development, which is independent of EDA-A1/EDAR/NF-κB signaling (Schmidt-Ullrich et al., 2001, 2006). During primary HF placode growth, E-cadherin downregulation must be independent of Snail because we did not detect any *Snai1* expression in our gene profiling analysis (Table S1), and a previous publication only revealed Snail protein expression at E16.5 (Jamora et al., 2005). By contrast *Snai3* was upregulated (1.6×) in primary hair placodes compared with interfollicular epidermis at E14.5 (Table S1), suggesting that it might substitute for Snail in primary hair placode growth.

Interestingly, *Tgfb2*-KO mice have a HF developmental phenotype that is very similar to that of *Lhx2*-KO mice (data not

Development (2016) 143, 1512-1522 doi:10.1242/dev.130898

shown; Fig. 4) (Foitzik et al., 1999). This prompted us to ask whether TGFβ signaling is affected in *Lhx2*-KO and *ΔN* embryonic skin at E14.5. In control embryos, TGFβ2 protein expression was detected in the suprabasal layer of the epidermis, in the entire placode border adjacent to the dermis and in the dermal condensate, the future dermal papilla (Fig. 4A, upper panels) (Jamora et al., 2005). Phospho-SMAD2 (pSMAD2) expression, which provides a sensitive read-out parameter for active TGFβ signaling, was observed in the entire epidermis, including HF placodes, and also in the dermal condensate of controls (Fig. 4A, upper panels). In *Lhx2*-KO embryos, TGFβ2 protein was still expressed in the suprabasal epidermis, but pSMAD2 expression was reduced at this site compared with controls (Fig. 4A, upper panels). In HF placodes and dermal condensates of *Lhx2*-KO embryos, pSMAD2 expression was strongly reduced and TGFβ2 protein expression was undetectable in both compartments at E14.5. Similarly to *Lhx2*-KOs, *ΔN* embryos only expressed TGFβ2 protein throughout the epidermis, but pSMAD2 expression was also strongly decreased (Fig. 4A, upper panels). However, qRT-PCR indicated that *Tgfb2* is not a direct target gene of either NF-κB or LHX2 in epidermis or dermis (Fig. 1C; Fig. 4C; Table S2). Furthermore, the *Tgfb2* gene lacks binding sites for NF-κB and LHX2 (Table S3). This suggests an indirect control of TGFβ2 protein expression and/or activity by NF-κB and LHX2 in placodes and dermal condensate.

In line with the findings described above, E-cadherin expression was absent in proximal placode borders of controls at E14.5, but was readily detectable in placodes of *Lhx2*-KO embryos (Fig. 4A, lower panels). As expected, in *ΔN* embryos E-cadherin expression was observed in the entire epidermis without local downregulation because primary HF placode formation is barely initiated and only reaches a rudimentary stage 0/1 (Fig. 4A, lower panels) (Schmidt-Ullrich et al., 2006; Zhang et al., 2009a). We also analyzed fibronectin 1 (Fn1) expression, which plays an important role in cell adhesion, migration and proliferation during embryonic development (Schwarzbauer and DeSimone, 2011). *Fn1* mRNA expression was upregulated in control placodes at E14.5 (Fig. 4B,D). By contrast, *Lhx2*-KO embryos revealed diminished *Fn1* mRNA expression and in *ΔN* embryos *Fn1* was not detected

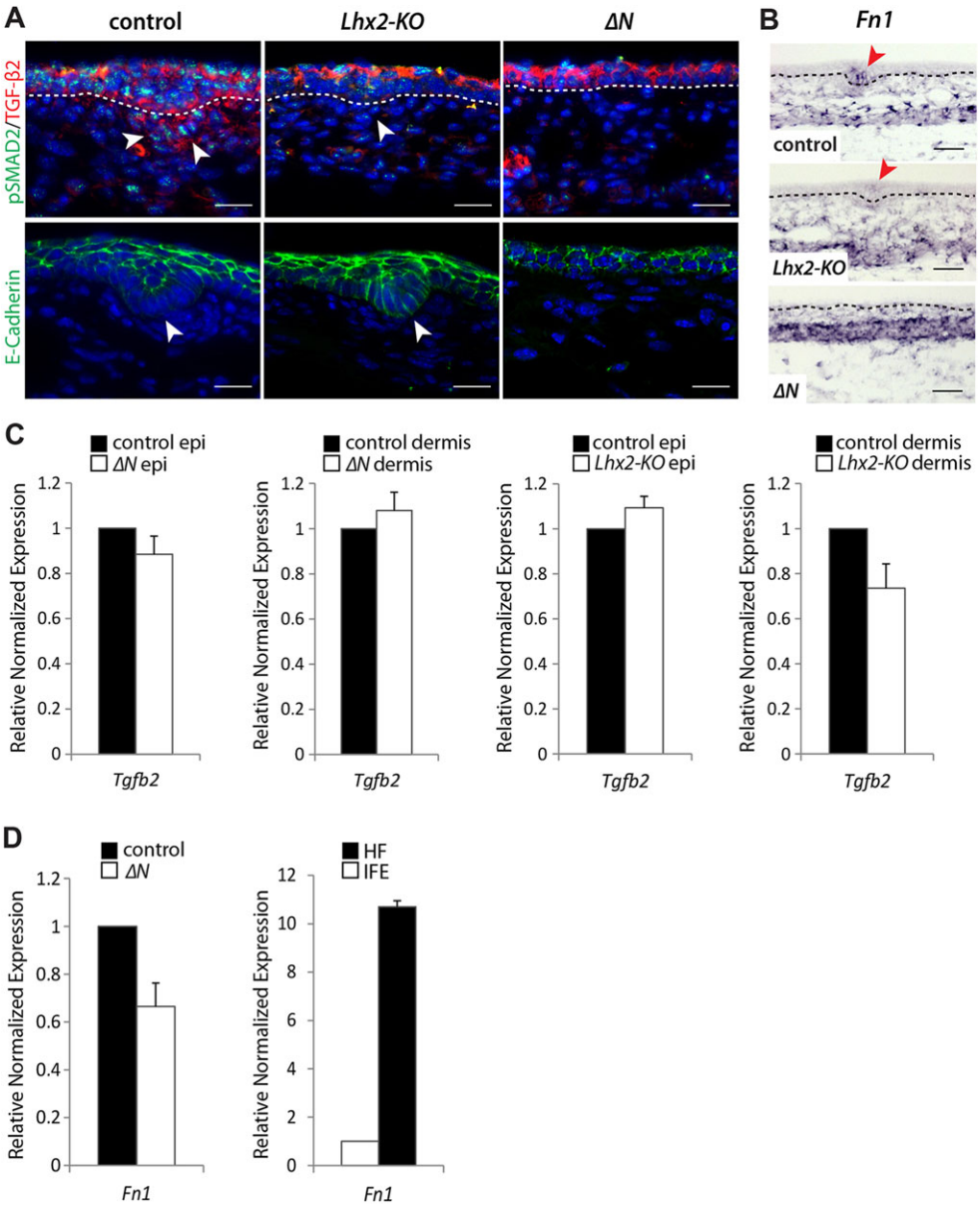

Fig. 4. *Lhx2*-KO mice exhibit delayed primary HF development and, as in *ΔN* mice, impaired TGFβ signaling and lack of E-cadherin downregulation. (A) Immunostaining on sagittal sections of *n*=3 control, *Lhx2*-KO and *ΔN* embryos at E14.5 using antibodies against anti-pSMAD2 (green), TGFβ2 (red) and E-cadherin (green). Arrowheads indicate presence or absence of pSMAD2 and TGFβ2 expression in the dermal papilla and of E-cadherin expression the HF placode; dashed line delineates dermal-epidermal boundaries. Blue, nuclear DAPI staining. (B) *In situ* hybridization for *Fn1* mRNA on sagittal sections of *n*=3 control, *Lhx2*-KO and *ΔN* embryos at E14.5. Arrowheads indicate *Fn1* mRNA expression in the HF placode; dashed line delineates dermal-epidermal boundaries. (C,D) qRT-PCR for *Tgfb2* (C) and *Fn1* (D) using mRNA isolated from epidermal keratinocytes of *n*=3 *ΔN*, *Lhx2*-KO or control embryos at E14.5. Data are presented as mean±s.e.m. Scale bars: 20 µm in A; 50 µm in B.

Development (2016) 143, 1512-1522 doi:10.1242/dev.130898

(Fig. 4B,D; see also Fig. 1C). Together, these findings suggest that delayed placode formation in *Lhx2*-KO mice and absent placode down-growth in *ΔN* mice are caused in part by decreased TGFβ2 signaling, failure of E-cadherin downregulation, and decreased Fn1 expression.

Recombinant TGFβ2 restores primary HF development in *Lhx2*-KO embryonic skin explants

As TGFβ2 signaling appears to function downstream of LHX2 in primary HF placode formation, we investigated whether primary placode growth in *Lhx2*-KO mice could be rescued by treatment of cultured E14.5 skin explants with recombinant TGFβ2. TGFβ2 treatment of E14.5 skin explants from control mice slightly accelerated primary HF placode growth and expression of cell migration and proliferation markers or E-cadherin downregulation (Fig. S4A,B), consistent with previously published data (Foitzik et al., 1999). TGFβ2-treated *Lhx2*-KO explants showed significantly increased formation of placodes at hair morphogenesis stages 1 and 2 after 24 h compared with untreated explants (Fig. 5A). TGFβ2 treatment of *Lhx2*-KO explants not only rescued and enhanced placode down-growth, but also restored TGFβ signaling, downregulation of E-cadherin and levels of the cell migration and proliferation markers pFAK and Ki67 in HF placodes (Fig. 5B). Thus, TGFβ2 activation acts downstream of LHX2 to promote transient E-cadherin downregulation. By contrast, treatment of *ΔN* skin explant cultures with recombinant TGFβ2 did not rescue HF development (Fig. S4A). This indicates that additional NF-κB targets, probably including growth regulators such as SHH, and/or physiological processes such as ECM remodeling (see above) are required downstream of NF-κB activity and cannot be compensated for by addition of TGFβ2 alone (Mill et al., 2003; Schmidt-Ullrich et al., 2006; St-Jacques et al., 1998; Zhang et al., 2009a).

DISCUSSION

Here, we identified a novel NF-κB/LHX2/TGFβ2 signaling axis that results in E-cadherin downregulation in primary HFs at early stages of their formation, an essential requirement for placode down-growth (summarized in Fig. 6) (Jamora et al., 2003, 2005; Zhang et al., 2009a). Several EDA-A-dependent target genes have previously been identified and shown to function in HF development. These targets support a function for EDA-A1/EDAR/NF-κB signaling in placode patterning, WNT regulation and BMP suppression, but do not elucidate its role in intrinsic down-growth mechanisms (Bazzi et al., 2007; Cui et al., 2002, 2006; Fliniaux et al., 2008; Lefebvre et al., 2012; Mou et al., 2006; Pummila et al., 2007; Zhang et al., 2009a). Another downstream NF-κB target, SHH, promotes placode growth by upregulating cyclin D1 expression (see Fig. 1C) (Mill et al., 2003; Pummila et al., 2007; Schmidt-Ullrich et al., 2006). However, this occurs well after induction of EDA-A1/EDAR/NF-κB signaling, consistent with the later arrest of follicle development in *Shh*-deficient compared with NF-κB-inhibited mice (Chiang et al., 1999; Schmidt-Ullrich et al., 2006; St-Jacques et al., 1998). In the current study, we therefore sought to identify NF-κB-dependent factors that are specifically required to establish the appropriate conditions for placode down-growth beyond initiation. Our data confirm an essential role for EDA-A1/EDAR/NF-κB signaling in preparing primary hair pre-placodes for down-growth and identify several novel NF-κB target genes. Importantly, we identified the LIM homeobox transcription factor LHX2 as a crucial new NF-κB-controlled gene that contributes to providing the proper conditions for placode down-growth primarily by activation of TGFβ2 signaling, a known hair placode growth inducer (summarized in Fig. 6) (Foitzik et al., 1999; Jamora et al., 2005).

We further show that NF-κB regulates genes involved in ECM remodeling (*Frem1*, *Mmp9*, *Tnc*), cell migration (*Nrp2*, *Prokr2*, *Cd74*) and adhesion (*Ncam1*, *Madcam1*) in primary hair placodes at E14.5. We have previously observed loss of structural organization at sites of placode induction when NF-κB activity is suppressed (Schmidt-Ullrich et al., 2006). This might be due in part to reorganization of the epidermis (Schmidt-Ullrich et al., 2006). The characteristic structural organization of epidermal keratinocytes and of the underlying dermal condensate at sites of placode formation is most likely an important prerequisite for

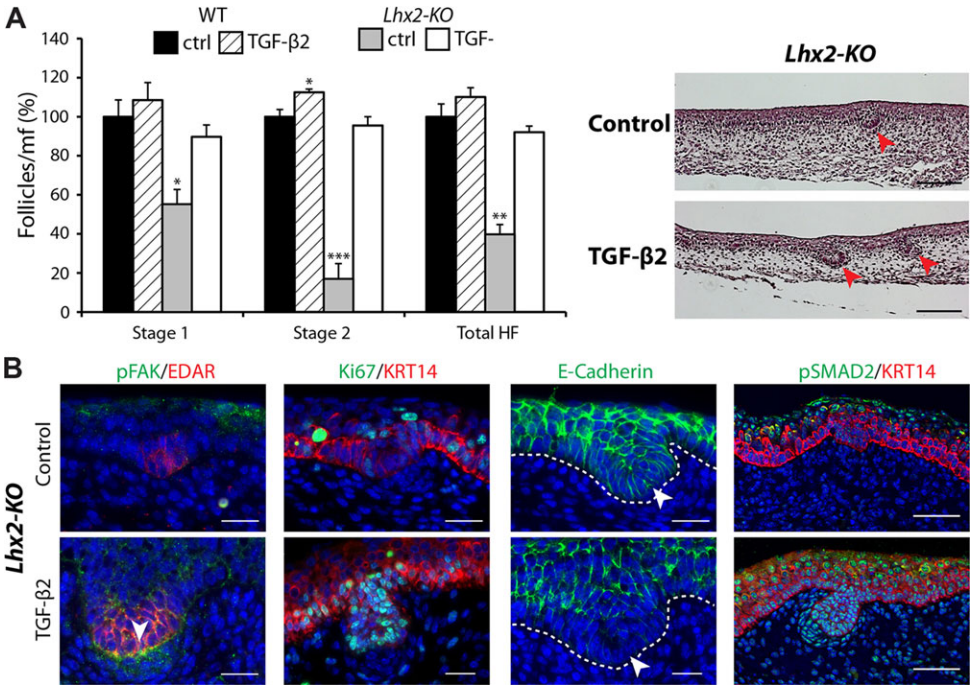

Fig. 5. Treatment of *Lhx2*-KO embryonic skin explants with TGFβ2 rescued proper primary HF development. (A) Embryonic skin explants of *n*=3 E14.5 control or *Lhx2*-KO mice were either left untreated (ctrl) or treated with recombinant TGFβ2 (100 ng/ml) for 24 h. Skin samples were stained with H&E (right), and follicles were quantified as percentage relative to the number of follicles per microscopic field in the control group (left). Statistical analyses were performed using two-tailed unpaired *t*-test. Data were pooled from three biological replicates and presented as mean±s.e.m. **P*<0.05; ***P*<0.01; ****P*<0.001. Arrowheads indicate HF placodes. Scale bars: 100 µm. (B) Immunostaining on *Lhx2*-KO explants treated with recombinant TGFβ2 or left untreated (control) using antibodies against pFAK, EDAR, Ki67, KRT14, E-cadherin and pSMAD2. Arrowheads indicate pFAK and the presence or absence of E-cadherin expression in the HF placode border; dashed line delineates dermal-epidermal boundaries. Blue, nuclear DAPI staining. Scale bars: 20 µm (pFAK, Ki67, E-cadherin); 50 µm (pSMAD2).

Development (2016) 143, 1512-1522 doi:10.1242/dev.130898

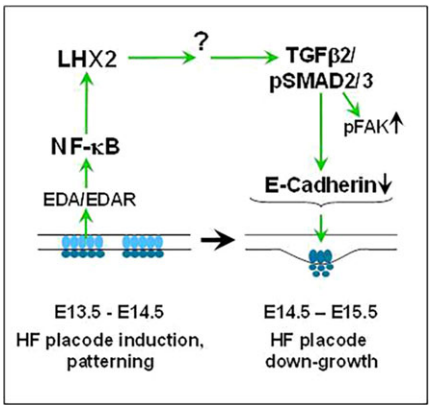

Fig. 6. Model for primary placode down-growth involving NF-κB signaling. We show here that LHX2 expression is directly regulated by EDA-A1/EDAR/NF-κB signaling, as NF-κB activity in primary placodes depends on EDA-A1/EDAR (Schmidt-Ullrich et al., 2006). By an as yet unknown mechanism LHX2 activates TGFβ2 signaling in primary HF placodes, which results in phosphorylation of FAK (pFAK), and, importantly, in downregulation of E-cadherin expression. Together, these results introduce a novel NF-κB/LHX2/TGFβ2 signaling axis that is required for establishing the proper conditions for placode down-growth, and might also be relevant for other epidermal-mesenchymal tissue interactions, for epithelial-mesenchymal transition or for tumor growth.

subsequent down-growth. It has also recently been suggested that EDA-A1/EDAR/NF-κB signaling is involved in modulating cell motility and placodal fate decisions resulting in early placode formation prior to down-growth, as mice with forced epidermal EDA-A1 expression displayed increased cell motility in the interfollicular epidermis and in future areas of HF formation (Ahtiainen et al., 2014). However, excess EDA-A1 expression generally results in premature and aberrant placode formation and, therefore, might not reflect the physiological role of endogenous EDA-A1 signaling in hair placode induction (Ahtiainen et al., 2014; Mustonen et al., 2003). Our detailed NF-κB-dependent gene signature in hair placodes supports a mandatory role for NF-κB signaling in ECM remodeling and cell migration and is consistent with our previous findings that NF-κB is required for placode pattern refinement and down-growth rather than rudimentary pre-placode formation and hair fate decisions, which are both dependent on canonical WNT signaling (Andl et al., 2002; Schmidt-Ullrich et al., 2006; Zhang et al., 2009a). Overall, our study illuminates a role for NF-κB in primary HF development that extends well beyond the previously described functions in terms of molecular controls in tissue remodeling, and might be relevant for understanding other epithelial-mesenchymal tissue interaction systems, such as those that occur in tumor growth.

After completion of our studies, an RNA-seq-based transcriptome of HF progenitors was published (Sennett et al., 2015) (see also http://hair-gel.net/). This useful resource confirms our findings regarding placode-specific expression of *Lhx2*, *Dkk4*, *Foxi3*, *Shh*, *Tnfaip*, *Wnt10b*, *Fgf20* and *Ascl4*. However, our *in situ* hybridization and qPCR studies revealed several inconsistencies, for instance regarding the location of *Fn1*, *Prokr2*, *Sox9*, *Nrp2*, *Frem1*, *Ncam1* and *Trps1* expression. The RNA-seq data of Sennett et al. indicate exclusive expression of these genes in the dermal compartment; however, our *in situ* hybridization and qPCR studies reveal that *Sox9*, *Prokr* and *Fn1* expression is confined to the hair placode, whereas *Nrp2*, *Frem1*, *Ncam1* and *Trps1* are expressed in both placode and dermal condensate (Fig. 1D,E; Fig. 2E,F; Fig. 4B; Fig. S3A-C). These discrepancies highlight the need to verify gene expression patterns inferred from FACS analyses and transcriptional profiling using independent approaches.

Our data suggest that EDA-A1/EDAR/NF-κB controls primary placode down-growth at various levels, including ECM remodeling, and downstream expression of LHX2, which leads to activation of TGFβ2 signaling and subsequent E-cadherin downregulation (Fig. 6). In terms of hair placode growth delay, *Lhx2*-KO mice strongly resemble mice deficient in *Tgfb2* expression (Fig. 2) (Foitzik et al., 1999), and, similarly to *Tgfb2*-KOs (Jamora et al., 2005), E-cadherin downregulation was absent in stage 1 placodes of *Lhx2*-KO embryos at E14.5. The importance of E-cadherin downregulation for hair placode down-growth, which is dependent on TGFβ2 signaling, was demonstrated previously using mice with forced epidermal E-cadherin expression in which placode growth was totally blocked (Jamora et al., 2003, 2005). Although neither NF-κB nor LHX2 appear to control expression of the *Tgfb2* gene or components of the pathway (Fig. 1; Fig. 4C,D; Table S1) (Folgueras et al., 2013), activation of TGFβ2 signaling is downstream of both transcription factors and directly or indirectly depends on the transcriptional activity of LHX2. As almost all cell types express TGFβ receptors, TGFβ activation is tightly controlled. The TGFβ protein is produced as a latent inactive form that is mainly activated by binding to integrins (Worthington et al., 2011). It is thus conceivable that NF-κB and particularly LHX2 are indirectly responsible for the release of TGFβ2 from its latent inactive form. Initiation of placode down-growth leads to changes in the ECM at the proximal placode border. These changes are likely to be controlled by NF-κB and downstream LHX2 (see above) and may make local integrins available for binding to latent TGFβ complexes. Another reason for lack of TGFβ2 activity in *ΔN* and *Lhx2*-KO mice might be loss of Nrp2 (neuropilin 2) expression in hair placodes of both mouse models. It was recently shown that neuropilins can activate the latent TGFβ complex (Glinka et al., 2011). Furthermore, neuropilins can act as co-receptors for TGFβ receptors and increase the response to latent and active TGFβ (Glinka et al., 2011). In *Lhx2*-KO mice, *Nrp2* mRNA expression was absent in the epidermis; however, it was still expressed in the dermal condensate, which may be sufficient to induce TGFβ signaling and placode down-growth when *Lhx2*-KO skin explants are treated with recombinant TGFβ2. Further investigation of the mechanisms by which NF-κB functions to mediate local changes in cell adhesion and ECM modulation in placode down-growth will be highly interesting in light of the important roles of NF-κB in tumor growth.

In mature follicles, LHX2 controls HF stem cell maintenance and proliferation by regulating cytoskeletal organization, polarity and cell adhesion within the niche (Folgueras et al., 2013; Mardaryev et al., 2011; Rhee et al., 2006). Placode growth also involves changes in cell adhesion, polarity and proliferation and we show that *Lhx2*-KO mice have delayed primary hair placode growth. Thus, in addition to its role in promoting TGFβ2 signaling, LHX2 might have some analogous functions in HF stem cell maintenance and in early primary placode down-growth. Exploring the molecular connections between embryonic HF precursors and adult stem cells will be a fascinating area for future studies.

MATERIALS AND METHODS

Generation of transgenic mice and animal experiments

All aspects of animal care and experimental protocols were approved by the Berlin Animal Review Board (Reg. G 0261/02, G 0077/08, G 0082/13 and X 9013/11). The *EGFP* cDNA was cloned immediately downstream of an artificial NF-κB-responsive promoter, which has been described previously

Development (2016) 143, 1512-1522 doi:10.1242/dev.130898

(Schmidt-Ullrich et al., 1996). The construct was linearized, purified and used for pronuclear microinjection to generate *B6-Tg(κ-EGFP)3Pt/Rsu* mice (here referred to as *κ-EGFP*). Pre-existing mouse strains used for this study have been described earlier: *129;129P2-ctnnb1$^{tm(NFKBIA\Delta N)1Rsu}$* (*ΔN*) (Schmidt-Ullrich et al., 2001), *B6-Lhx2^{tm1Hwe}* (*Lhx2* knockout mice, here referred to as *Lhx2*-KO, were kindly provided by H. Westphal) (Porter et al., 1997) and *B6CBACa-A^{w-J}/A-Ta* (*tabby*, *ta/ta*) (*Eda-A1*-mutant mice, kindly provided by I. Thesleff) (Falconer, 1952). Mice and embryos were genotyped by PCR of genomic DNA. Heterozygous *Lhx2*-KO mice were crossbred to obtain homozygous mutants, which were collected before E16.5.

Isolation of primary placode keratinocytes by flow cytometry

Back skin from E14.5 *κ-EGFP* embryos was dissected and treated overnight with dispase (BD Biosciences; 2.5 units/ml) at 4°C, which selectively separated the epidermis with primary placodes from the underlying dermis. The epidermal fraction was treated with 10 mM EDTA, and cell suspensions were subsequently strained (35-µm pores; BD Biosciences). Further purification of placode keratinocytes was performed using a FACSAria III system, equipped with FACS DiVa software (BD Biosciences). Cells were gated for single events and viability, and then sorted by EGFP expression. Purity of the sorted placode keratinocyte population was determined by post-sort FACS analysis and typically exceeded 95% (Fig. S1). Back skin from E14.5 *κ-EGFP* embryos of various different litters was prepared this way and pooled for five independent microarray experiments.

Microarray and qRT-PCR

Total RNA from either epidermal keratinocytes of five control or five *ΔN* embryos at E14.5, or of FACS-purified EGFP-positive (placode) or EGFP-negative (IFE) epidermal keratinocytes from *κ-EGFP* embryos at E14.5 (see above) was isolated using the Absolutely RNA Microprep Kit (Agilent Technologies) and then processed with the WT Expression Kit (Ambion) and the WT Terminal Labeling and Hybridization Kit (Affymetrix). Processed RNA was hybridized to the Mouse Gene 1.0 ST Array (Affymetrix). Five biological replicates for each sample were analyzed statistically with the multi-factor ANOVA test using Partek Genomic Suites software (Partek). The complete microarray data are listed in Table S1. For quantitative real-time PCR (qRT-PCR), total RNA was used to generate cDNA by means of the iScript cDNA Synthese Kit (Bio-Rad). qRT-PCR primers were designed using Primer3 software (see Table S2). See supplementary Materials and Methods for primer sequences. Reactions were performed in triplicate using the GoTaq qPCR Master Mix (Promega) and a CFX 96 real-time PCR detection system (Bio-Rad). Differences between samples were calculated using the CFX Manager software (Bio-Rad) based on the ΔΔCt equitation method, and were normalized to three house-keeping genes (*Actb*, *Gapdh* and *Hmbs*). Statistical significance was estimated using unpaired Student's *t*-test.

Histology, immunofluorescence and *in situ* hybridization

Back skin samples were fixed in 4% paraformaldehyde/MEM or in Bouin's fixative overnight at 4°C, and were either directly embedded in Tissue Tek O.C.T. or dehydrated and paraffin-embedded. Routine Hematoxylin and Eosin (H&E) staining was performed for morphological evaluation. The progress of HF development was assessed by morphometry using the classification of HF stages by Hardy (1992) and Paus et al. (1999). Cryosections were used for cytoskeleton staining with Phalloidin coupled to Alexa Fluor 488 (Life Technologies, 1:100). Immunofluorescence and *in situ* hybridization on paraffin sections were performed as described previously (Zhang et al., 2009a). Antibodies and dilutions used were: rat anti-P-cadherin (Invitrogen, 13-2000Z; 1:400); chicken anti-EGFP (Abcam, ab13970; 1:1600); goat anti-LHX2 (Santa Cruz Biotechnology, Sc-19344; 1:400); rabbit and chicken anti-KRT14 (Convance, AF64 and CK14; 1:2000); goat anti-EDAR (R&D Systems, AF745; 1:200); rabbit anti-pSMAD2 (Cell Signaling, #3101; 1:400); rabbit anti-phospho-FAK (Y397) (Santa Cruz, sc-11765R; 1:400); rabbit anti-Ki67 (Abcam, ab15580; 1:400); mouse anti-E-cadherin (BD Biosciences, #610181; 1:100); mouse anti-TGFβ2 (Abcam, ab36495; 1:100); digoxigenin-conjugated sheep anti-AP Fab fragments (Roche, #11093274910; 1:1000).

Probe sequences used for *in situ* hybridization are provided in the supplementary Materials and Methods. Images were obtained by a conventional or confocal Zeiss microscope.

Chromatin immunoprecipitation (ChIP)

One million EGFP-positive (placode) or EGFP-negative (IFE) epidermal keratinocytes from E14.5 *κ-EGFP* embryos were fixed in 1% formaldehyde for 10 min at room temperature. Subsequent cell lysis, sonification and ChIP assays were performed using the MAGnify Chromatin Immunoprecipitation System (Invitrogen). For each immunoprecipitation, cells were incubated with 6 µg rabbit anti-NF-κB p65 (RelA) antibody (Santa Cruz, sc-372 X). qRT-PCR was then performed to visualize specific enrichment of potential NF-κB binding regions. Ct values of the region of interest and a control region (transcription start site of *Gapdh*) were measured in the input and ChIP sample, and ΔCt values were calculated. Three replicates were measured and mean± s.e.m. was calculated. Statistical analysis was performed using unpaired Student's *t*-test. Primers are listed in supplementary Materials and Methods.

Embryonic skin culture

Back skin explants from *Lhx2*-KO and control littermates were collected at E14.5, transferred onto 0.1 µm PVDF membranes (Millipore) and cultured using Advanced DMEM:F12 (Gibco) supplemented with 0.5 mM L-glutamine and 100 units/ml penicillin/streptomycin. Skins were kept in a floating culture. Explants were either treated with 100 ng/ml human recombinant TGFβ2 (PeproTech) or left untreated. After 24 h, explants were harvested and prepared for paraffin embedding (see above). Progression of HF development was monitored in three independent biological replicates. For each replicate, the number of placode and germ stage follicles per microscopic field (100×) was calculated in 30 H&E-stained sections. *P*-values were calculated using unpaired Student's *t*-test.

Acknowledgements

We thank Sandra Herms, Inge Krahn, Doris Lange, Vivian Schulz, Lisa Spatt and Sarah Ugowski for excellent technical help and animal welfare and breeding; Heiner Westphal for *Lhx2*-KO mice; Irma Thesleff for *Ta*/*Ta* mice; Ronald Naumann for transgenic mouse production; and Hans-Peter Rahn (FACS) and Gabriele Born (MCF core facility, MDC) for technical assistance.

Competing interests

The authors declare no competing or financial interests.

Author contributions

P.T. designed and performed the experiments, and analyzed the data. R.P. designed experiments, analyzed the data and edited the manuscript. S.E.M. analyzed the data and edited the manuscript. C.S. analyzed the data and edited the manuscript. R.S.-U. oversaw the entire project, designed experiments, analyzed the data and wrote the paper.

Funding

This work was funded by grants from the German Research Foundation (Deutsche Forschungsgemeinschaft, DFG) [SCHM 855/3-3 to R.S.-U. and PA 345/13-3 to R.P.].

Data availability

Microarray data have been deposited in ArrayExpress under accession numbers E-MTAB-4534 (gene expression in total epidermis of E14.5 mouse embryos with blocked NF-κB pathway) and E-MTAB-4535 (primary hair placode profiling).

Supplementary information

Supplementary information available online at
http://dev.biologists.org/lookup/suppl/doi:10.1242/dev.130898/-/DC1

References

Ahtiainen, L., Lefebvre, S., Lindfors, P. H., Renvoisé, E., Shirokova, V., Vartiainen, M. K., Thesleff, I. and Mikkola, M. L. (2014). Directional cell migration, but not proliferation, drives hair placode morphogenesis. *Dev. Cell* **28**, 588-602.

Andl, T., Reddy, S. T., Gaddapara, T. and Millar, S. E. (2002). WNT signals are required for the initiation of hair follicle development. *Dev. Cell* **2**, 643-653.

Bazzi, H., Fantauzzo, K. A., Richardson, G. D., Jahoda, C. A. B. and Christiano, A. M. (2007). The Wnt inhibitor, Dickkopf 4, is induced by canonical Wnt signaling during ectodermal appendage morphogenesis. *Dev. Biol.* **305**, 498-507.

Biggs, L. C. and Mikkola, M. L. (2014). Early inductive events in ectodermal appendage morphogenesis. *Semin. Cell Dev. Biol.* **25-26**, 11-21.
Botchkarev, V. A., Botchkareva, N. V., Roth, W., Nakamura, M., Chen, L.-H., Herzog, W., Lindner, G., McMahon, J. A., Peters, C., Lauster, R. et al. (1999). Noggin is a mesenchymally derived stimulator of hair-follicle induction. *Nat. Cell Biol.* **1**, 158-164.
Botchkareva, N. V., Botchkarev, V. A., Chen, L.-H., Lindner, G. and Paus, R. (1999). A role for p75 neurotrophin receptor in the control of hair follicle morphogenesis. *Dev. Biol.* **216**, 135-153.
Bulchand, S., Grove, E. A., Porter, F. D. and Tole, S. (2001). LIM-homeodomain gene Lhx2 regulates the formation of the cortical hem. *Mech. Dev.* **100**, 165-175.
Chen, D., Jarrell, A., Guo, C., Lang, R. and Atit, R. (2012). Dermal beta-catenin activity in response to epidermal Wnt ligands is required for fibroblast proliferation and hair follicle initiation. *Development* **139**, 1522-1533.
Chiang, C., Swan, R. Z., Grachtchouk, M., Bolinger, M., Litingtung, Y., Robertson, E. K., Cooper, M. K., Gaffield, W., Westphal, H., Beachy, P. A. et al. (1999). Essential role for Sonic hedgehog during hair follicle morphogenesis. *Dev. Biol.* **205**, 1-9.
Cui, C.-Y., Durmowicz, M., Tanaka, T. S., Hartung, A. J., Tezuka, T., Hashimoto, K., Ko, M. S. H., Srivastava, A. K. and Schlessinger, D. (2002). EDA targets revealed by skin gene expression profiles of wild-type, Tabby and Tabby EDA-A1 transgenic mice. *Hum. Mol. Genet.* **11**, 1763-1773.
Cui, C.-Y., Hashimoto, T., Grivennikov, S. I., Piao, Y., Nedospasov, S. A. and Schlessinger, D. (2006). Ectodysplasin regulates the lymphotoxin-beta pathway for hair differentiation. *Proc. Natl. Acad. Sci. USA* **103**, 9142-9147.
de Oliveira, K. A., Kaergel, E., Heinig, M., Fontaine, J. F., Patone, G., Muro, E. M., Mathas, S., Hummel, M., Andrade-Navarro, M. A., Hübner, N. and Scheidereit, C. (2016). A roadmap of constitutive NF-κB activity in Hodgkin lymphoma: dominant roles of p50 and p52 revealed by genome-wide analyses. *Genome Med.* **8**, 28. doi:10.1186/s13073-016-0280-5.
Essayem, S., Kovacic-Milivojevic, B., Baumbusch, C., McDonagh, S., Dolganov, G., Howerton, K., Larocque, N., Mauro, T., Ramirez, A., Ramos, D. M. et al. (2006). Hair cycle and wound healing in mice with a keratinocyte-restricted deletion of FAK. *Oncogene* **25**, 1081-1089.
Falconer, D. S. (1952). A totally sex-linked gene in the house mouse. *Nature* **169**, 664-665.
Fantauzzo, K. A., Bazzi, H., Jahoda, C. A. B. and Christiano, A. M. (2008a). Dynamic expression of the zinc-finger transcription factor Trps1 during hair follicle morphogenesis and cycling. *Gene Expr. Patterns* **8**, 51-57.
Fantauzzo, K. A., Tadin-Strapps, M., You, Y., Mentzer, S. E., Baumeister, F. A. M., Cianfarani, S., Van Maldergem, L., Warburton, D., Sundberg, J. P. and Christiano, A. M. (2008b). A position effect on TRPS1 is associated with Ambras syndrome in humans and the Koala phenotype in mice. *Hum. Mol. Genet.* **17**, 3539-3551.
Fliniaux, I., Mikkola, M. L., Lefebvre, S. and Thesleff, I. (2008). Identification of dkk4 as a target of Eda-A1/Edar pathway reveals an unexpected role of ectodysplasin as inhibitor of Wnt signalling in ectodermal placodes. *Dev. Biol.* **320**, 60-71.
Foitzik, K., Paus, R., Doetschman, T. and Dotto, G. P. (1999). The TGF-beta2 isoform is both a required and sufficient inducer of murine hair follicle morphogenesis. *Dev. Biol.* **212**, 278-289.
Folgueras, A. R., Guo, X., Pasolli, H. A., Stokes, N., Polak, L., Zheng, D. and Fuchs, E. (2013). Architectural niche organization by LHX2 is linked to hair follicle stem cell function. *Cell Stem Cell* **13**, 314-327.
Frame, M. C., Patel, H., Serrels, B., Lietha, D. and Eck, M. J. (2010). The FERM domain: organizing the structure and function of FAK. *Nat. Rev. Mol. Cell Biol.* **11**, 802-814.
Fuchs, E. (2007). Scratching the surface of skin development. *Nature* **445**, 834-842.
Glinka, Y., Stoilova, S., Mohammed, N. and Prud'homme, G. J. (2011). Neuropilin-1 exerts co-receptor function for TGF-beta-1 on the membrane of cancer cells and enhances responses to both latent and active TGF-beta. *Carcinogenesis* **32**, 613-621.
Hardy, M. H. (1992). The secret life of the hair follicle. *Trends Genet.* **8**, 55-61.
Headon, D. J. and Overbeek, P. A. (1999). Involvement of a novel Tnf receptor homologue in hair follicle induction. *Nat. Genet.* **22**, 370-374.
Hirota, J. and Mombaerts, P. (2004). The LIM-homeodomain protein Lhx2 is required for complete development of mouse olfactory sensory neurons. *Proc. Natl. Acad. Sci. USA* **101**, 8751-8755.
Jamora, C., DasGupta, R., Kocieniewski, P. and Fuchs, E. (2003). Links between signal transduction, transcription and adhesion in epithelial bud development. *Nature* **422**, 317-322.
Jamora, C., Lee, P., Kocieniewski, P., Azhar, M., Hosokawa, R., Chai, Y. and Fuchs, E. (2005). A signaling pathway involving TGF-beta2 and snail in hair follicle morphogenesis. *PLoS Biol.* **3**, e11.
Jiang, T.-X., Widelitz, R. B., Shen, W.-M., Will, P., Wu, D.-Y., Lin, C.-M., Jung, H.-S. and Chuong, C.-M. (2004). Integument pattern formation involves genetic and epigenetic controls: feather arrays simulated by digital hormone models. *Int. J. Dev. Biol.* **48**, 117-135.
Johnson, J.-L. F. A., Hall, T. E., Dyson, J. M., Sonntag, C., Ayers, K., Berger, S., Gautier, P., Mitchell, C., Hollway, G. E. and Currie, P. D. (2012). Scube activity is necessary for Hedgehog signal transduction in vivo. *Dev. Biol.* **368**, 193-202.
Kadaja, M., Keyes, B. E., Lin, M., Pasolli, H. A., Genander, M., Polak, L., Stokes, N., Zheng, D. and Fuchs, E. (2014). SOX9: a stem cell transcriptional regulator of secreted niche signaling factors. *Genes Dev.* **28**, 328-341.
Kere, J., Srivastava, A. K., Montonen, O., Zonana, J., Thomas, N., Ferguson, B., Munoz, F., Morgan, D., Clarke, A., Baybayan, P. et al. (1996). X-linked anhidrotic (hypohidrotic) ectodermal dysplasia is caused by mutation in a novel transmembrane protein. *Nat. Genet.* **13**, 409-416.
Kiso, M., Tanaka, S., Saba, R., Matsuda, S., Shimizu, A., Ohyama, M., Okano, H. J., Shiroishi, T., Okano, H. and Saga, Y. (2009). The disruption of Sox21-mediated hair shaft cuticle differentiation causes cyclic alopecia in mice. *Proc. Natl. Acad. Sci. USA* **106**, 9292-9297.
Kumar, A., Eby, M. T., Sinha, S., Jasmin, A. and Chaudhary, P. M. (2001). The ectodermal dysplasia receptor activates the nuclear factor-kappaB, JNK, and cell death pathways and binds to ectodysplasin A. *J. Biol. Chem.* **276**, 2668-2677.
Kunath, M., Lüdecke, H.-J. and Vortkamp, A. (2002). Expression of Trps1 during mouse embryonic development. *Gene Expr. Patterns* **2**, 119-122.
Laurikkala, J., Pispa, J., Jung, H. S., Nieminen, P., Mikkola, M., Wang, X., Saarialho-Kere, U., Galceran, J., Grosschedl, R. and Thesleff, I. (2002). Regulation of hair follicle development by the TNF signal ectodysplasin and its receptor Edar. *Development* **129**, 2541-2553.
Le Bail, O., Schmidt-Ullrich, R. and Israel, A. (1993). Promoter analysis of the gene encoding the I kappa B-alpha/MAD3 inhibitor of NF-kappa B: positive regulation by members of the rel/NF-kappa B family. *EMBO J.* **12**, 5043-5049.
Lefebvre, S., Fliniaux, I., Schneider, P. and Mikkola, M. L. (2012). Identification of ectodysplasin target genes reveals the involvement of chemokines in hair development. *J. Invest. Dermatol.* **132**, 1094-1102.
Lettice, L. A., Williamson, I., Wiltshire, J. H., Peluso, S., Devenney, P. S., Hill, A. E., Essafi, A., Hagman, J., Mort, R., Grimes, G. et al. (2012). Opposing functions of the ETS factor family define Shh spatial expression in limb buds and underlie polydactyly. *Dev. Cell* **22**, 459-467.
Malik, T. H., von Stechow, D., Bronson, R. T. and Shivdasani, R. A. (2002). Deletion of the GATA domain of TRPS1 causes an absence of facial hair and provides new insights into the bone disorder in inherited tricho-rhino-phalangeal syndromes. *Mol. Cell. Biol.* **22**, 8592-8600.
Mangale, V. S., Hirokawa, K. E., Satyaki, P. R. V., Gokulchandran, N., Chikbire, S., Subramanian, L., Shetty, A. S., Martynoga, B., Paul, J., Mai, M. V. et al. (2008). Lhx2 selector activity specifies cortical identity and suppresses hippocampal organizer fate. *Science* **319**, 304-309.
Mao, J., McGlinn, E., Huang, P., Tabin, C. J. and McMahon, A. P. (2009). Fgf-dependent Etv4/5 activity is required for posterior restriction of Sonic Hedgehog and promoting outgrowth of the vertebrate limb. *Dev. Cell* **16**, 600-606.
Mardaryev, A. N., Meier, N., Poterlowicz, K., Sharov, A. A., Sharova, T. Y., Ahmed, M. I., Rapisarda, V., Lewis, C., Fessing, M. Y., Ruenger, T. M. et al. (2011). Lhx2 differentially regulates Sox9, Tcf4 and Lgr5 in hair follicle stem cells to promote epidermal regeneration after injury. *Development* **138**, 4843-4852.
Mill, P., Mo, R., Fu, H., Grachtchouk, M., Kim, P. C. W., Dlugosz, A. A. and Hui, C.-C. (2003). Sonic hedgehog-dependent activation of Gli2 is essential for embryonic hair follicle development. *Genes Dev.* **17**, 282-294.
Momeni, P., Glöckner, G., Schmidt, O., von Holtum, D., Albrecht, B., Gillessen-Kaesbach, G., Hennekam, R., Meinecke, P., Zabel, B., Rosenthal, A. et al. (2000). Mutations in a new gene, encoding a zinc-finger protein, cause tricho-rhino-phalangeal syndrome type I. *Nat. Genet.* **24**, 71-74.
Mou, C., Jackson, B., Schneider, P., Overbeek, P. A. and Headon, D. J. (2006). Generation of the primary hair follicle pattern. *Proc. Natl. Acad. Sci. USA* **103**, 9075-9080.
Mustonen, T., Pispa, J., Mikkola, M. L., Pummila, M., Kangas, A. T., Pakkasjärvi, L., Jaatinen, R. and Thesleff, I. (2003). Stimulation of ectodermal organ development by Ectodysplasin-A1. *Dev. Biol.* **259**, 123-136.
Nowak, J. A., Polak, L., Pasolli, H. A. and Fuchs, E. (2008). Hair follicle stem cells are specified and function in early skin morphogenesis. *Cell Stem Cell* **3**, 33-43.
Oro, A. E. and Scott, M. P. (1998). Splitting hairs: dissecting roles of signaling systems in epidermal development. *Cell* **95**, 575-578.
Paus, R., Muller-Rover, S., Van Der Veen, C., Maurer, M., Eichmuller, S., Ling, G., Hofmann, U., Foitzik, K., Mecklenburg, L. and Handjiski, B. (1999). A comprehensive guide for the recognition and classification of distinct stages of hair follicle morphogenesis. *J. Invest. Dermatol.* **113**, 523-532.
Porter, F. D., Drago, J., Xu, Y., Cheema, S. S., Wassif, C., Huang, S. P., Lee, E., Grinberg, A., Massalas, J. S., Bodine, D. et al. (1997). Lhx2, a LIM homeobox gene, is required for eye, forebrain, and definitive erythrocyte development. *Development* **124**, 2935-2944.
Pummila, M., Fliniaux, I., Jaatinen, R., James, M. J., Laurikkala, J., Schneider, P., Thesleff, I. and Mikkola, M. L. (2007). Ectodysplasin has a dual role in ectodermal organogenesis: inhibition of Bmp activity and induction of Shh expression. *Development* **134**, 117-125.
Rhee, H., Polak, L. and Fuchs, E. (2006). Lhx2 maintains stem cell character in hair follicles. *Science* **312**, 1946-1949.

Schaller, M. D. (2010). Cellular functions of FAK kinases: insight into molecular mechanisms and novel functions. *J. Cell Sci.* **123**, 1007-1013.
Schmidt-Ullrich, R. and Paus, R. (2005). Molecular principles of hair follicle induction and morphogenesis. *Bioessays* **27**, 247-261.
Schmidt-Ullrich, R., Memet, S., Lilienbaum, A., Feuillard, J., Raphael, M. and Israel, A. (1996). NF-kappaB activity in transgenic mice: developmental regulation and tissue specificity. *Development* **122**, 2117-2128.
Schmidt-Ullrich, R., Aebischer, T., Hulsken, J., Birchmeier, W., Klemm, U. and Scheidereit, C. (2001). Requirement of NF-kappaB/Rel for the development of hair follicles and other epidermal appendices. *Development* **128**, 3843-3853.
Schmidt-Ullrich, R., Tobin, D. J., Lenhard, D., Schneider, P., Paus, R. and Scheidereit, C. (2006). NF-kappaB transmits Eda A1/EdaR signalling to activate Shh and cyclin D1 expression, and controls post-initiation hair placode down growth. *Development* **133**, 1045-1057.
Schneider, M. R., Schmidt-Ullrich, R. and Paus, R. (2009). The hair follicle as a dynamic miniorgan. *Curr. Biol.* **19**, R132-R142.
Schober, M., Raghavan, S., Nikolova, M., Polak, L., Pasolli, H. A., Beggs, H. E., Reichardt, L. F. and Fuchs, E. (2007). Focal adhesion kinase modulates tension signaling to control actin and focal adhesion dynamics. *J. Cell Biol.* **176**, 667-680.
Schwarzbauer, J. E. and DeSimone, D. W. (2011). Fibronectins, their fibrillogenesis, and in vivo functions. *Cold Spring Harb. Perspect. Biol.* **3**, a005041.
Sennett, R. and Rendl, M. (2012). Mesenchymal–epithelial interactions during hair follicle morphogenesis and cycling. *Semin. Cell Dev. Biol.* **23**, 917-927.
Sennett, R., Wang, Z., Rezza, A., Grisanti, L., Roitershtein, N., Sicchio, C., Mok, K. W., Heitman, N. J., Clavel, C., Ma'ayan, A. et al. (2015). An integrated transcriptome atlas of embryonic hair follicle progenitors, their niche, and the developing skin. *Dev. Cell* **34**, 577-591.
Shetty, A. S., Godbole, G., Maheshwari, U., Padmanabhan, H., Chaudhary, R., Muralidharan, B., Hou, P.-S., Monuki, E. S., Kuo, H.-C., Rema, V. et al. (2013). Lhx2 regulates a cortex-specific mechanism for barrel formation. *Proc. Natl. Acad. Sci. USA* **110**, E4913-E4921.
Shirokova, V., Jussila, M., Hytönen, M. K., Perälä, N., Drögemüller, C., Leeb, T., Lohi, H., Sainio, K., Thesleff, I. and Mikkola, M. L. (2013). Expression of Foxi3 is regulated by ectodysplasin in skin appendage placodes. *Dev. Dyn.* **242**, 593-603.
Sick, S., Reinker, S., Timmer, J. and Schlake, T. (2006). WNT and DKK determine hair follicle spacing through a reaction-diffusion mechanism. *Science* **314**, 1447-1450.
Sieg, D. J., Hauck, C. R., Ilic, D., Klingbeil, C. K., Schaefer, E., Damsky, C. H. and Schlaepfer, D. D. (2000). FAK integrates growth-factor and integrin signals to promote cell migration. *Nat. Cell Biol.* **2**, 249-256.
St-Jacques, B., Dassule, H. R., Karavanova, I., Botchkarev, V. A., Li, J., Danielian, P. S., McMahon, J. A., Lewis, P. M., Paus, R. and McMahon, A. P. (1998). Sonic hedgehog signaling is essential for hair development. *Curr. Biol.* **8**, 1058-1069.
Sulzmaier, F. J., Jean, C. and Schlaepfer, D. D. (2014). FAK in cancer: mechanistic findings and clinical applications. *Nat. Rev. Cancer* **14**, 598-610.
Takeuchi, M. and Baichwal, V. R. (1995). Induction of the gene encoding mucosal vascular addressin cell adhesion molecule 1 by tumor necrosis factor alpha is mediated by NF-kappa B proteins. *Proc. Natl. Acad. Sci. USA* **92**, 3561-3565.
Törnqvist, G., Sandberg, A., Hägglund, A.-C. and Carlsson, L. (2010). Cyclic expression of lhx2 regulates hair formation. *PLoS Genet.* **6**, e1000904.
Tsao, K.-C., Tu, C.-F., Lee, S.-J. and Yang, R.-B. (2013). Zebrafish scube1 (signal peptide-CUB (complement protein C1r/C1s, Uegf, and Bmp1)-EGF (epidermal growth factor) domain-containing protein 1) is involved in primitive hematopoiesis. *J. Biol. Chem.* **288**, 5017-5026.
Vidal, V. P. I., Chaboissier, M.-C., Lützkendorf, S., Cotsarelis, G., Mill, P., Hui, C.-C., Ortonne, N., Ortonne, J.-P. and Schedl, A. (2005). Sox9 is essential for outer root sheath differentiation and the formation of the hair stem cell compartment. *Curr. Biol.* **15**, 1340-1351.
Worthington, J. J., Klementowicz, J. E. and Travis, M. A. (2011). TGFbeta: a sleeping giant awoken by integrins. *Trends Biochem. Sci.* **36**, 47-54.
Yan, M., Wang, L.-C., Hymowitz, S. G., Schilbach, S., Lee, J., Goddard, A., de Vos, A. M., Gao, W.-Q. and Dixit, V. M. (2000). Two-amino acid molecular switch in an epithelial morphogen that regulates binding to two distinct receptors. *Science* **290**, 523-527.
Yoon, S., Woo, S. U., Kang, J. H., Kim, K., Shin, H.-J., Gwak, H.-S., Park, S. and Chwae, Y.-J. (2012). NF-kappaB and STAT3 cooperatively induce IL6 in starved cancer cells. *Oncogene* **31**, 3467-3481.
Yoshizaki, T., Sato, H., Furukawa, M. and Pagano, J. S. (1998). The expression of matrix metalloproteinase 9 is enhanced by Epstein-Barr virus latent membrane protein 1. *Proc. Natl. Acad. Sci. USA* **95**, 3621-3626.
Zhang, Y., Andl, T., Yang, S. H., Teta, M., Liu, F., Seykora, J. T., Tobias, J. W., Piccolo, S., Schmidt-Ullrich, R., Nagy, A. et al. (2008). Activation of {beta}-catenin signaling programs embryonic epidermis to hair follicle fate. *Development* **135**, 2161-2172.
Zhang, Y., Tomann, P., Andl, T., Gallant, N. M., Huelsken, J., Jerchow, B., Birchmeier, W., Paus, R., Piccolo, S., Mikkola, M. L. et al. (2009a). Reciprocal requirements for EDA/EDAR/NF-kappaB and Wnt/beta-catenin signaling pathways in hair follicle induction. *Dev. Cell* **17**, 49-61.
Zhang, Z., Verheyden, J. M., Hassell, J. A. and Sun, X. (2009b). FGF-regulated Etv genes are essential for repressing Shh expression in mouse limb buds. *Dev. Cell* **16**, 607-613.